Nearly ferromagnetic Fermi-liquid behaviour in YFe_2Zn_{20} and high-temperature ferromagnetism of $GdFe_2Zn_{20}$

S. JIA[1], S. L. BUD'KO[1], G. D. SAMOLYUK[2] AND P. C. CANFIELD[1]*

[1]Ames Laboratory US DOE and Department of Physics and Astronomy, Iowa State University, Ames, Iowa 50011, USA

[2]Ames Laboratory US DOE and Department of Chemistry, Iowa State University, Ames, Iowa 50011, USA

*e-mail: canfield@ameslab.gov

Published online: 25 March 2007; doi:10.1038/nphys568

One of the historic goals of alchemy was to turn base elements into precious ones. Although the practice of alchemy has been superseded by chemistry and solid-state physics, the desire to dramatically change or tune the properties of a compound, preferably through small changes in stoichiometry or composition, remains. This desire becomes even more compelling for compounds that can be tuned to extremes in behaviour. Here, we report that the RT_2Zn_{20} (R = rare earth and T = transition metal) family of compounds manifests exactly this type of versatility, even though they are more than 85% Zn. By tuning T, we find that YFe_2Zn_{20} is closer to ferromagnetism than elemental Pd, the classic example of a nearly ferromagnetic Fermi liquid. By submerging Gd in this highly polarizable Fermi liquid, we tune the system to a remarkably high-temperature ferromagnetic ($T_C = 86$ K) state for a compound with less than 5% Gd. Although this is not quite turning lead into gold, it is essentially tuning Zn to become a variety of model compounds.

The field of condensed-matter physics has been interested in the effects of electron correlations from its inception[1,2]. To this day, the properties of elemental Fe as well as Pd continue to present problems that interest both experimentalists as well as theorists[3]. Materials such as Pd or Pt, that are just under the Stoner limit (often referred to as nearly ferromagnetic Fermi liquids), or materials just over the Stoner limit, such as $ZrZn_2$ or Sc_3In on the ferromagnetic side, are of particular interest[1–3]. Of even greater interest are new examples of nearly ferromagnetic Fermi liquids that can be tuned with a greater degree of ease than the pure elements: that is, those that can accommodate controlled substitutions on a number of unique crystallographic sites in a manner that allows for (1) a tuning of the band filling/Fermi surface and (2) the introduction of local-moment-bearing ions onto a unique crystallographic site. Such a versatile system would open the field to a greater range of experimental studies of strongly correlated electronic states as well as potentially allowing for more detailed studies of quantum criticality and possibly even novel superconducting states.

Here, we present our first results of an extensive study of the dilute, rare-earth-bearing, intermetallic series RT_2Zn_{20} (R = rare earth and T = transition metal) that supports a wide range of R ions for T in and near the Fe, Co and Ni columns of the periodic table. In particular, we will show how YFe_2Zn_{20} is an archetypical example of a nearly ferromagnetic Fermi liquid and how, by embedding Gd ions into this highly polarizable medium, $GdFe_2Zn_{20}$ can have a remarkably high ferromagnetic ordering temperature of 86 K, even though it contains less than 5% atomic Gd and the Fe is not moment-bearing in the paramagnetic state.

The RT_2Zn_{20} series of compounds was discovered in 1997 by Nasch *et al.*[4] and is isostructural to the cubic $CeCr_2Al_{20}$ structure ($Fd\bar{3}m$ space group)[5,6]. The rare-earth and transition-metal ions each occupy their own single, unique crystallographic sites (8*a* and 16*d* respectively), whereas the Zn ions have three unique crystallographic sites (96*g*, 48*f* and 16*c*). In addition, the rare-earth site is one of cubic point symmetry ($\bar{4}3m$). The coordination polyhedra for R and T consist fully of Zn, meaning that there are no R–R, T–T or R–T nearest neighbours and the shortest R–R spacing is ~6 Å. The lattice parameters for the series are ~14 Å. Although the crystallography of this series was well detailed, so far, there have been no measurements of these compounds' physical properties. This, to some extent, is not unexpected because the limited data sets available on the RT_2Al_{20} compounds[6,7] indicated very low ordering temperatures, consistent with the very low R concentrations.

Figures 1 and 2 show the temperature-dependent electrical resistivity, specific heat and low-field magnetization data, as well as anisotropic $M(H)$ data, for $GdFe_2Zn_{20}$ and $GdCo_2Zn_{20}$. There are two conspicuous differences between the physical properties of these compounds: (1) $GdFe_2Zn_{20}$ orders ferromagnetically, whereas $GdCo_2Zn_{20}$ orders antiferromagnetically and (2) $GeFe_2Zn_{20}$ orders at a remarkably high temperature of $T_C = 86$ K, whereas $GdCo_2Zn_{20}$ orders at the more representative $T_N = 5.7$ K. From Fig. 2a, the high-temperature Curie constant can be determined, giving effective moments ($8.05\mu_B$ and $8.15\mu_B$ for T = Fe and T = Co respectively) consistent with the effective moment of Gd^{3+}, indicating that, in the paramagnetic state, there is little or no contribution from the transition metal. The saturated moment deduced from the data in Fig. 2b is close to that associated with Gd^{3+}; slightly lower for $GdFe_2Zn_{20}$ and slightly higher for $GdCo_2Zn_{20}$. The magnetic entropy associated with each phase transition is approximately $R\ln 8$ (where R is the gas constant), with more uncertainty associated with the subtraction of the YT_2Zn_{20} data for T = Fe than for T = Co owing to the much higher ordering temperature. The remarkably high ordering temperature found for $GdFe_2Zn_{20}$ is not unique to the R = Gd member of the RFe_2Zn_{20} series. For R = Gd–Tm, transitions to ferromagnetically ordered states occur at temperatures that roughly scale with the de Gennes

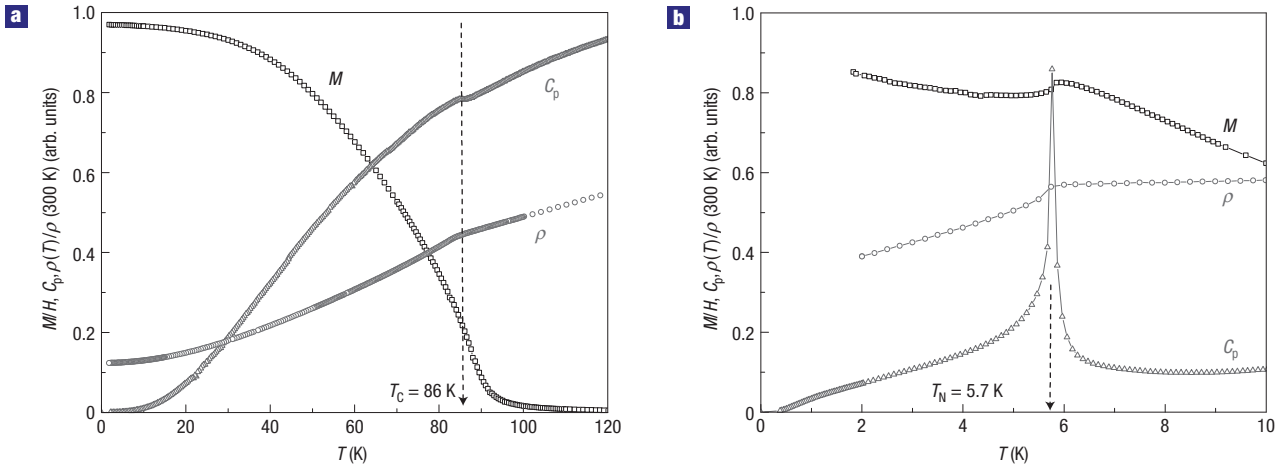

Figure 1 Temperature-dependent specific heat, resistivity and low-field ($H = 1{,}000$ Oe) magnetization divided by applied field for two GdT_2Zn_{20} compounds. **a**, $GdFe_2Zn_{20}$; the full scale represents 30 e.m.u. mol^{-1}, 500 J mol^{-1} K^{-1} and 1.0 for M/H, specific heat (C_p) and normalized electrical resistivitiy ($\rho(T)/\rho(300\,K)$), respectively. **b**, $GdCo_2Zn_{20}$; the full scale represents 1.4 e.m.u. mol^{-1}, 50 J mol^{-1} K^{-1} and 0.20 for M/H, C_p and $\rho(T)/\rho(300\,K)$, respectively. For $GdFe_2Zn_{20}$, $\rho(300\,K) = 73\,\mu\Omega$ cm and for $GdCo_2Zn_{20}$, $\rho(300\,K) = 60\,\mu\Omega$ cm.

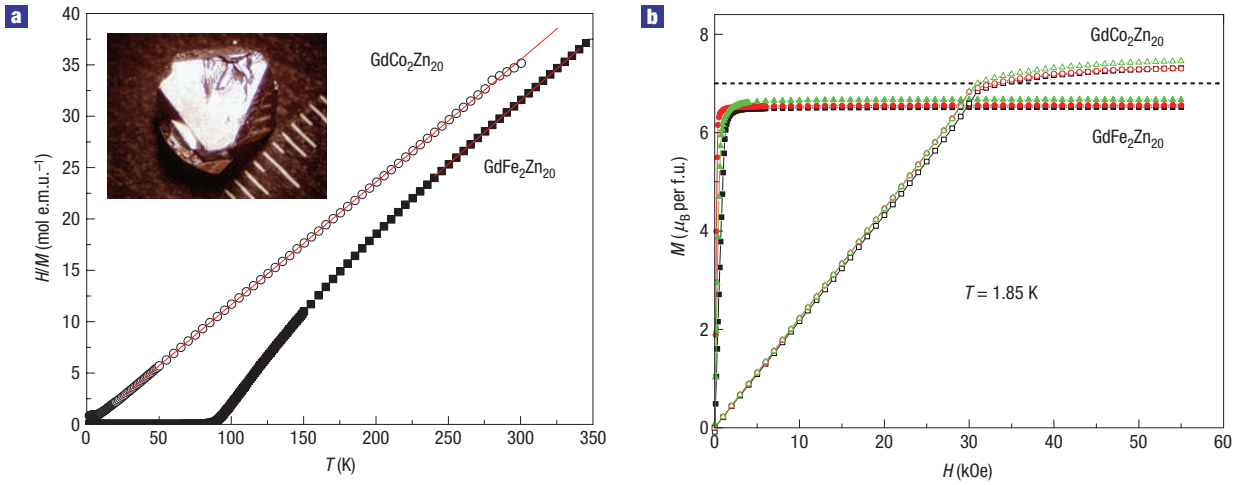

Figure 2 Magnetic properties of $GdFe_2Zn_{20}$ and $GdCo_2Zn_{20}$ compounds. **a**, H/M as a function of T (the lines show the region used for the high-temperature Curie–Weiss fit). Inset: A single crystal of YFe_2Zn_{20} next to a millimetre scale. **b**, Anisotropic $M(H)$ ($T = 1.85$ K). For each sample, measurements for $H \parallel [100]$, $H \parallel [110]$ and $H \parallel [111]$ are shown.

parameter ($T_C \approx 86, 57, 46, 29, 11, 5$ K for R = Gd, Tb, Dy, Ho, Er, Tm respectively).

To better understand this conspicuous difference in ordering temperatures, band-structure calculations were carried out. Figure 3 shows the density of states as a function of energy for both $LuFe_2Zn_{20}$ and $LuCo_2Zn_{20}$. The upper curve in each panel shows the total density of states, whereas the lower curve shows the density of states associated with the transition-metal ion. It should be noted that the difference between $LuFe_2Zn_{20}$ and $LuCo_2Zn_{20}$ density of states can be rationalized in terms of the rigid band approximation, with the Fermi level for $LuCo_2Zn_{20}$ being ~0.3 eV higher than that for $LuFe_2Zn_{20}$, associated with the two extra electrons per formula unit. Calculations done on YFe_2Zn_{20} and $GdFe_2Zn_{20}$ as well as on YCo_2Zn_{20} and $GdCo_2Zn_{20}$ lead to similar density of states curves and further analysis of the $GdFe_2Zn_{20}$ and $GdCo_2Zn_{20}$band-structural results leads to the prediction that for $GdFe_2Zn_{20}$ the ground state will be ferromagnetic with a total saturated moment of approximately $6.8\mu_B$ (with a small induced moment on the Fe opposing the Gd moment) and for $GdCo_2Zn_{20}$ the saturated moment will be $7.15\mu_B$ (with practically no induced moment on Co). These results are consistent with the saturated values of the magnetization seen in Fig. 2b.

These calculations indicate that the RFe_2Zn_{20} compounds should manifest a higher electronic density of states at the Fermi level, $N(E_F)$, than the RCo_2Zn_{20} analogues and raise the question of whether or not this is the primary reason for the remarkably high T_C found for $GdFe_2Zn_{20}$. In addition, they raise the question of how correlated the electronic state is in the nominally non-magnetic Lu- or Y-based analogues. To address these questions, two substitutional series were grown: $Y(Fe_xCo_{1-x})_2Zn_{20}$ and

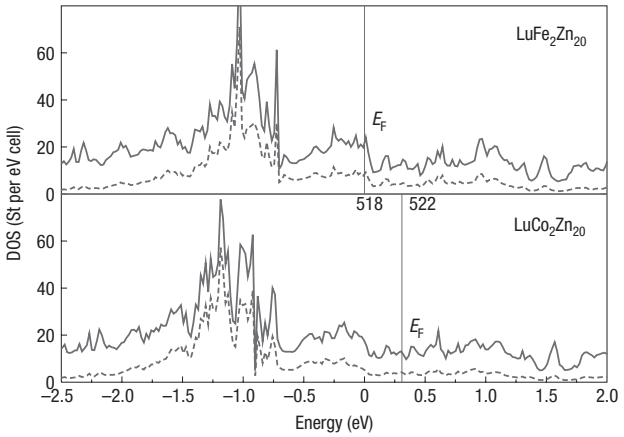

Figure 3 Density of states as a function of energy for $LuFe_2Zn_{20}$ and $LuCo_2Zn_{20}$. The upper curve shows total density, whereas the lower curve shows the partial density of states associated with Fe or Co.

$Gd(Fe_xCo_{1-x})_2Zn_{20}$. Figure 4 shows thermodynamic data taken on the $Y(Fe_xCo_{1-x})_2Zn_{20}$ series. For $x = 0$, the low-temperature, linear component of the specific heat (γ) is relatively small ($19\,mJ\,mol^{-1}\,K^{-2}$) and the susceptibility is weakly paramagnetic and essentially temperature independent. As x is increased, there is a monotonic (but clearly super-linear) increase in the samples' paramagnetism as well as, for larger x values, an increase in the low-temperature γ values. For YFe_2Zn_{20} ($x = 1$), the value of γ has increased to over 250% of that for YCo_2Zn_{20} and the susceptibility has become both large and temperature dependent. Figure 5 shows data on the analogous $Gd(Fe_xCo_{1-x})_2Zn_{20}$ series. As x is increased, the ground state rapidly becomes ferromagnetic (only $x = 0$ was antiferromagnetic) and the transition temperature increases monotonically (but again in a super-linear fashion) and the high-field, saturated magnetization decreases weakly, in a monotonic fashion.

Taken together, Figs 4 and 5 demonstrate a clear correlation between x, the linear component of the electronic specific heat, the enhanced magnetic susceptibility of the Y-based series and the Curie temperature and the saturated magnetization of the Gd-based series. This correlation can be more clearly seen if the relation between the linear component of the specific heat and the low-temperature susceptibility of the Y-based series is placed in the context of a nearly ferromagnetic Fermi liquid: that is, if the Stoner enhancement parameter, Z, for each member of the series can be determined[8]. For such systems, the static susceptibility (corrected for the core diamagnetism[9]) is $\chi = \chi_0/(1-Z)$, where $\chi_0 = \mu_B N(E_F)$. Given that the linear component of the specific heat is given by $\gamma_0 = (\pi k_B)^2 N(E_F)/3$, if both the low-temperature specific heat and magnetic susceptibility can be measured, then the parameter Z can be deduced ($Z = 1 - (3\mu_B{}^2/\pi^2 k_B{}^2)(\gamma_0/\chi_0)$), where k_B and μ_B are the Boltzmann constant and the Bohr magneton respectively. The canonical example of such a system is elemental Pd for which, using data from ref. 10, $Z = 0.83$. For YFe_2Zn_{20}, $Z = 0.89$, a value that places it even closer to the Stoner limit than Pd. It should be noted that the temperature-dependent susceptibility of YFe_2Zn_{20} is also remarkably similar to that of Pd (see ref. 3 and references therein). The x dependence of the experimentally determined values of γ and $\chi(T = 0)$, as well as the inferred value of Z, for the $Y(Fe_xCo_{1-x})_2Zn_{20}$ series is plotted in Fig. 4c. By choosing x, $Y(Fe_xCo_{1-x})_2Zn_{20}$ can be tuned from being exceptionally close to the Stoner limit to being well removed

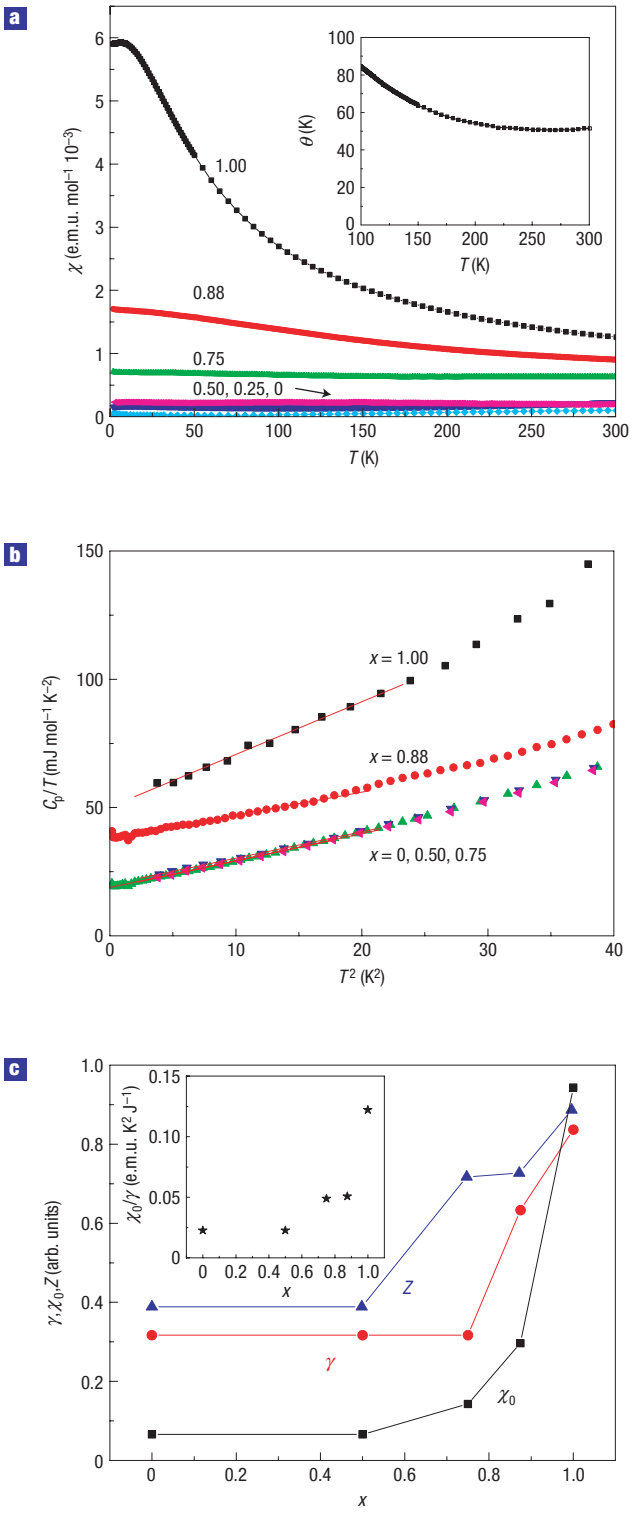

Figure 4 Thermodynamic properties of the $Y(Fe_xCo_{1-x})_2Zn_{20}$ series. **a**, Temperature-dependent magnetic susceptibility. Inset: Temperature dependence of paramagnetic Θ for $GdFe_2Zn_{20}$ (see text). **b**, Low-temperature C/T as a function of T^2. **c**, Linear coefficient of the specific heat, γ, magnetic susceptibility for $T \to 0$ corrected for core diamagnetism (-2.3×10^{-4} e.m.u. mol^{-1} for $Y(Fe_xCo_{1-x})_2Zn_{20}$ using table 5.7 (p. 306) of ref. 9), χ_0, and Stoner enhancement factor, Z, as a function of Fe concentration, x. The full scale represents 60 mJ mol^{-1} K^{-2}, 6.5×10^{-3} e.m.u. mol^{-1} and 1.0 for γ, χ_0 and Z respectively. Inset: Ratio χ_0/γ versus x.

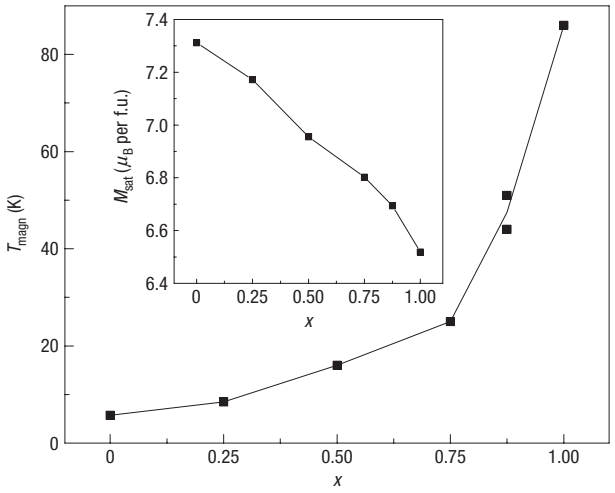

Figure 5 Magnetic ordering temperature in the $Gd(Fe_xCo_{1-x})_2Zn_{20}$ series as a function of Fe concentration x. Note that data from two samples of $x = 0.88$ are shown. Inset: M_{sat} as a function of x Fe.

from it. Corrections to these inferred Z values coming from the difference between the measured electronic specific heat coefficient, γ, and the Sommerfeld coefficient, γ_0, where $\gamma = \gamma_0(1 + \lambda)$ only serves to slightly increase Z because λ, the electron mass enhancement parameter, is positive definite. By comparing the γ_0 inferred from the band structure to our measured values of γ, we can estimate $\lambda = 0.85$ and 0.22 for $x = 1$ and $x = 0$ respectively, and this shifts Z to 0.94 for YFe_2Zn_{20} and to 0.50 for YCo_2Zn_{20}. The Wilson ratio, R, which is proportional to χ_0/γ apparently increases drastically approaching the Fe end in the $Y(Fe_xCo_{1-x})_2Zn_{20}$ series (Fig. 4c, inset).

When the non-magnetic Y ion is replaced by the large Heisenberg moment associated with the $S = 7/2$ Gd^{3+} ion, as x is varied from zero to one in the $Gd(Fe_xCo_{1-x})_2Zn_{20}$ series, the Gd local moments will be in an increasingly polarizable matrix, one that is becoming a nearly ferromagnetic Fermi liquid. This results in an increasingly strong coupling between the Gd local moments as x is increased. Figure 5 shows the x dependence of T_C and μ_{sat} for the $Gd(Fe_xCo_{1-x})_2Zn_{20}$. The value of T_C increases in a monotonic but highly nonlinear fashion in a manner reminiscent of the behaviour associated with the increasingly polarizability of $Y(Fe_xCo_{1-x})_2Zn_{20}$ seen in Fig. 4c. The μ_{sat} value for the field applied along the [111] direction varies systematically from the slightly enhanced value of 7.3 μ_B found for $GdCo_2Zn_{20}$ to the slightly deficient value of 6.5 μ_B found for $GdFe_2Zn_{20}$.

In addition to x dependence, this conceptually simple and compelling framework can also be used to understand the rather curious temperature dependence of the $1/\chi$ versus T data for $GdFe_2Zn_{20}$ seen in Fig. 2a. As T is decreased, the electronic background that the Gd^{3+} ion is immersed in becomes increasingly polarizable (as shown in Fig. 4a for $x = 1$), leading to a temperature-dependent coupling that in turn leads to the nonlinearity of the $1/\chi$ versus T data. If a constant effective moment for the Gd^{3+} is assumed, then a temperature-dependent, paramagnetic Θ can be extracted from the data in Fig. 2a: $\chi(T) = \chi_0 + C/(T - \Theta)$. This temperature-dependent Θ, shown in Fig. 4a, tracks the electronic susceptibility of the YFe_2Zn_{20} remarkably well, both increasing by ~1.7 on cooling from 300 to 100 K.

One consequence of placing Gd ions into a matrix so close to the Stoner limit is an enhanced sensitivity to small sample-to-sample variations. This is most clearly illustrated by the data for the $Gd(Fe_{0.88}Co_{0.12})_2Zn_{20}$ samples shown in Fig. 5. Although the samples have the same nominal composition, there is a clear difference in their transition temperatures. However, this difference is not too significant given the large dT_C/dx slope seen in Fig. 5. On the other hand, measurements on four separate samples of $Gd(Fe_{0.25}Co_{0.75})_2Zn_{20}$ did not show any significant variations in T_C. Such sensitivity of correlated electron states to small disorder is not uncommon, giving rise to significant variation in measured T_C for samples of Sc_3In and $ZrZn_2$ (ref. 1) as well as dramatic changes in the transport properties of heavy fermions such as $YbNi_2B_2C$ (refs 11–13).

The broader RT_2Zn_{20} family of compounds offers an even larger phase space for the study of correlated electron physics (for T = Fe, Ru and Os as well as for R = Yb and Ce)[14] and for the study of local-moment physics, all in the limit of a dilute, rare-earth-bearing, intermetallic series. The study of these compounds is a topic of ongoing research and promises to be a fruitful new phase space for several years to come.

METHODS

Single crystals of RFe_2Zn_{20}, RCo_2Zn_{20} and $R(Fe_xCo_{1-x})_2Zn_{20}$ (R = Gd, Y) were grown from high-temperature solutions[15] rich in Zn using initial compositions of $R_2T_4Zn_{94}$. The constituent elements were placed in an alumina crucible, sealed in a quartz ampule under ~1/3 atmosphere Ar and heated in a box furnace to 1,000 °C and then slowly cooled to 600 °C over up to 100 h. The resulting single crystals were large and often manifested clear [111] facets (see Fig. 2a, inset). For $R(Fe_xCo_{1-x})_2Zn_{20}$, x values are nominal values, but these are confirmed by elemental analysis as well as compliance with Vegard's law, with the lattice parameter varying linearly between the $x = 0$ and 1 end points. Field- and temperature-dependent magnetization measurements were made using Quantum Design magnetic property measurement system units, whereas transport and specific-heat measurements were made using Quantum Design physical property measurement system units with ^{3}He options. The electronic band structure was calculated using the atomic sphere approximation tight-binding linear muffin-tin orbital method[16,17] within the local density approximation with Barth–Hedin[18] exchange correlation using the experimental values of the lattice parameters. The number of atoms in the reduced unit cell is 46. A mesh of 16 **k** points in the irreducible part of the Brillouin zone was used. The 4*f* electrons of Gd and Lu atoms were treated as core states (polarized in the case of Gd atoms).

Received 28 November 2006; accepted 29 January 2007; published 25 March 2007.

References

1. Moriya, T. *Spin Fluctuations in Itinerant Electron Magnetism* (Springer, Berlin, 1985).
2. Brommer, P. E. & Franse, J. J. M. in *Ferromagnetic Materials* Vol. 5 (eds Buschow, K. H. J. & Wohlfarth, E. P.) 224 (Elsevier, Amsterdam, 1990).
3. Zellermann, B., Paintner, A. & Voitländer, J. The Onsager reaction field concept applied to the temperature dependent magnetic susceptibility of the enhanced paramagnets Pd and Pt. *J. Phys. Condens. Matter* **16**, 919–934 (2004).
4. Nasch, T., Jeitschko, W. & Rodewald, U. C. Ternary rare earth transition metal zinc compounds RT_2Zn_{20} with T = Fe, Ru, Co, Rh, and Ni. *Z. Naturforsch. B* **52**, 1023–1030 (1997).
5. Kripyakevich, P. I. & Zarechnyuk, O. S. RCr_2Al_{20} compounds in systems of rare earth metals and calcium, and their crystal structures. *Dopov. Akad. Nauk Ukr. RSR, Ser. A* **30**, 364–367 (1968).
6. Thiede, V. M. T., Jeitschko, W., Niemann, S. & Ebel, T. $EuTa_2Al_{20}$, $Ca_6W_4Al_{43}$ and other compounds with $CeCr_2Al_{20}$ and $Ho_6Mo_4Al_{43}$ type structures and some magnetic properties of these compounds. *J. Alloys Compounds* **267**, 23–31 (1998).
7. Moze, O., Tung, L. D., Franse, J. J. M. & Buschow, K. H. J. Crystal structure and magnetic properties of CeV_2Al_{20} and $CeCr_2Al_{20}$. *J. Alloys Compounds* **268**, 39–41 (1998).
8. Ziman, J. E. *Principles of the Theory of Solids* 2nd edn (Cambridge Univ. Press, Cambridge, 1972).
9. Mulay, L. N. & Boudreaux, E. A. *Theory and Applications of Molecular Diamagnetism* (Wiley, New York, 1976).
10. Chouteau, G., Fourneaux, R., Gobrecht, K. & Tournier, R. Specific heat and susceptibility enhancement in dilute palladium:nickel alloys. *Phys. Rev. Lett.* **20**, 193–195 (1968).
11. Avila, M. A., Bud'ko, S. L. & Canfield, P. C. Drastic annealing effects in transport properties of single crystals of the $YbNi_2B_2C$ heavy fermion system. *Phys. Rev. B* **66**, 132504 (2002).
12. Avila, M. A. *et al.* Anomalous temperature-dependent transport in $YbNi_2B_2C$ and its correlation to microstructural features. *Phys. Rev. B* **69**, 2051077 (2004).
13. Bud'ko, S. L. & Canfield, P. C. Tuning the Hall coefficient in single crystals of the heavy fermion compound $YbNi_2B_2C$ by annealing. *Phys. Rev. B* **71**, 024409 (2005).
14. Torikachvili, M. S. *et al.* YbT_2Zn_{20} (T = Fe, Co, Ru, Rh, Os, Ir): Effects of degeneracy on six closely related heavy fermion compounds. Preprint at <http://arxiv.org/abs/cond-mat/0608422> (2006).

15. Canfield, P. C. & Fisk, Z. Growth of single crystals from metallic fluxes. *Phil. Mag. B* **65**, 1117–1123 (1992).
16. Andersen, O. K. Linear methods in band theory. *Phys. Rev. B* **12**, 3060–3083 (1975).
17. Andersen, O. K. & Jepsen, O. Explicit, first-principles tight-binding theory. *Phys. Rev. Lett.* **53**, 2571–2574 (1984).
18. von Barth, U. & Hedin, L. Local exchange-correlation potential for the spin-polarized case. *J. Phys. C* **5**, 1629–1642 (1972).

Acknowledgements

We are indebted to the following students and magneticians: K. Dennis, N. Ni, J. Friedrich, S. A. Law, H. Ko, E. D. Mun and A. Safa-Sefat for help in sample growth and characterization and J. Schmalian and B. N. Harmon for useful discussions. We also acknowledge D. Hall for his role in this publication. Ames Laboratory is operated for the US Department of Energy by Iowa State University under Contract No. W-7405-Eng.-82. This work was supported by the Director for Energy Research, Office of Basic Energy Sciences.
Correspondence and requests for materials should be addressed to P.C.C.

Author contributions

S.J., S.L.B. and P.C.C. contributed to experimental work and data analysis and G.D.S. contributed to band-structure calculations and data analysis.

Competing financial interests

The authors declare no competing financial interests.